

BIOINSPIRED SELF-HEALING COMPOSITE MATERIALS FOR SPACE AND AEROSPACE APPLICATIONS

R. Trask¹, I. Bond¹, G. Williams¹, H. Williams¹ and C. Semprimoschnig²

¹Department of Aerospace Engineering, University of Bristol, Queen's Building, University Walk, Bristol. BS8 1TR. U.K.

²European Space Agency, ESTEC, Materials Physics & Chemistry Section
PO BOX 299, Keplerlaan 1, NL - 2200 AG Noordwijk, The Netherlands.

ABSTRACT

The healing potential and repair strategies of living organisms is increasingly of interest to composite designers seeking lower mass structures with increased service life who wish to progress from a conventional damage tolerance philosophy. Naturally occurring 'materials' have evolved into highly sophisticated, integrated, hierarchical structures that commonly exhibit multifunctional behaviour. Inspiration from and mimicry of these microstructures and micromechanisms offers considerable potential for the design and improvement of composite material performance. The work presented in this paper considers bioinspired self-healing using resin filled hollow fibres embedded within composite laminates and biomimetic vascular networks embedded in composite sandwich structures. The work undertaken has shown healing efficiencies of >80% in flexure in both glass-fibre and carbon-fibre reinforced composite laminates and healing efficiencies of 100% in composite sandwich structures.

1. SELF-HEALING COMPOSITE MATERIALS

Advances in materials technologies have been largely responsible for major performance improvements in many engineering structures and continue to be key in determining the reliability, performance and cost effectiveness of such systems. Lightweight, high strength, high stiffness fibre reinforced polymer (FRP) composite materials are leading contenders to improve the efficiency and sustainability of many forms of transport. In addition, they offer immense scope for incorporating multifunctionality due to their hierarchical internal architecture. One limiting factor in their wider exploitation is relatively poor performance under impact loading, a crucial aspect of any safety critical design, leading to a significant reduction in strength, stiffness and stability.

For example, carbon fibre reinforced plastic (CFRP) used in aerospace applications is typically assigned an allowable strain level of <0.4% [1,2] whereas commercially available carbon fibres typically have a strain to failure of around 1.5%. This results in conservative design and higher weight structures. The inability to plastically deform results in energy absorption via the creation of matrix cracks and delaminations which can be difficult to detect visually. Self-healing has the potential to mitigate damage resulting from an impact event, thereby providing an opportunity to improve the design allowables for fibre reinforced polymers or offer

other benefits such as reduced maintenance and inspection schedules.

Conceptual inspiration from nature is not new, and many engineering approaches can be considered to have been inspired by observing natural systems. The healing potential and repair strategies of living organisms is increasingly of interest to designers seeking lower mass structures with increased service life who wish to progress from a conventional damage tolerance philosophy. Naturally occurring 'materials' have evolved into highly sophisticated, integrated, hierarchical structures that commonly exhibit multifunctional behaviour [3]. Inspiration and mimicry of these microstructures and micromechanisms offers considerable potential in the design and improvement of material performance [4] but many of the biological processes involved are extremely complex. Bioinspired self-healing using hollow fibres embedded within a structure has been investigated at different length scales in several materials by various authors, e.g. bulk concrete [5-7] bulk polymers [4, 8], and polymer composites [9-12]. The latter has seen exciting developments in recent years, for example [13-21], using the inspiration of biological self-healing applied with broadly traditional engineering approaches.

Hollow glass fibres [22, 23] are used in preference to embedded microcapsules [24, 25] because they offer the advantage of being able to store functional agents for self-repair as well as integrating easily with and acting as a reinforcement. A typical hollow fibre self-healing approach used within composite laminates could take the form of fibres containing a one-part resin system, a two-part resin and hardener system or a resin system with a catalyst or hardener contained within the matrix material [12].

A bespoke hollow glass fibre (HGF) making facility [22, 23] has been used to produce HGF between 30-100µm diameter with a hollowness of around 50%, Figure 1. These are then embedded within either glass fibre reinforced plastic (GFRP) or CFRP and infused with uncured resin to impart a self-healing functionality to the laminate. During a damage event some of these hollow fibres will fracture, thus, initiating the recovery of properties by 'healing' whereby a repair agent passes from within any broken hollow fibres to infiltrate the damage zone and acts to ameliorate the critical effects of matrix cracking and delamination between plies and, most importantly, prevent further damage propagation. This release of repair agent mimics the bleeding mechanism in biological organisms (e.g. Human Thrombosis).

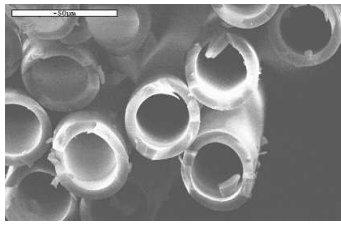


FIG.1 Hollow glass fibres manufactured at University of Bristol, UK.

The exact nature of the self-healing method will depend upon (1) the nature and location of the damage, (2) the choice of repair resin, and (3) the influence of the operational environment. The self-healing fibres can be introduced within a laminate as additional plies at each interface, at damage critical interfaces or as individual filaments spaced at predetermined distances within each ply. In order to more fully understand and optimise the healing process, two parallel studies were undertaken in glass reinforced and carbon reinforced epoxy systems respectively. A translucent glass/epoxy laminate provides good visualisation of damage occurrence and the healing process when viewed with transmission microscopy, however, a carbon/epoxy laminate is opaque and therefore, to enhance visualisation, an UV fluorescent dye (Ardrox 985) was added to the healing resin in both studies.

The discussion so far has been on the application of spaced single hollow fibres within a composite laminate. However, self-healing approaches and self-healing in mammals employ a biomimetic vascular network, which can be considered as an advance on existing liquid based healing approaches. For example, a vascular network offers the advantages of addressing larger damage volume, allowing multiple healing events and allowing replenishment of the system.

Sandwich structures offer very high specific flexural stiffness by using high performing skin materials, such as glass or carbon fibre composite, separated by a lightweight core. This makes them an attractive design option in aerospace and marine applications. Impact damage can degrade the flexural strength of composite sandwich structures by over 50% due to a loss of skin support inducing localised skin buckling. The space offered by the internal core of the sandwich structure offers the possibility of delivering a healing agent from a remote reservoir to a region of damage via a vascular network. This concept, as well as the hollow glass fibres will now be discussed.

2. SPECIMEN MANUFACTURE

2.1. Self-healing GFRP laminates

The HGF chosen for this study had an external diameter of $60 \mu\text{m} \pm 3 \mu\text{m}$ and an internal diameter of $\sim 40 \mu\text{m}$ yielding a hollowness fraction (ratio of internal to external area) of $\sim 55\%$. This larger fibre diameter (compared to Figure 2) gives a greater volume for healing agent storage. Once manufactured the individual fibres were consolidated within a 913 epoxy resin film (42gsm), which was selected to match the baseline laminate material. The healing resin can then be infused into the individual

filaments using a vacuum assisted capillary action. Once the ends have been sealed (Bostik BondFlex 100HMA high modulus silicone sealant) the infused hollow fibre layers (which can now be considered as standard 'prepreg' plies) are incorporated into a laminate stacking sequence as required, and processed according to the resin film manufacturer's guidelines.

A 16 ply composite laminate with a $[0^\circ/+45^\circ/90^\circ/-45^\circ]_2s$ stacking sequence manufactured from pre-impregnated E-glass/913 epoxy resin (Hexcel Composites) was selected for the first evaluation of the HGF self-healing approach. Self-healing filaments were introduced at four $0^\circ/45^\circ$ damage critical ply interfaces that were identified and reported previously [21], as shown in Figure 3. An epoxy resin system (CYTEC Cycom 823) was selected as the healing resin because of the need to match the chemistry of the host laminate, it's availability as a two-part system permitting inclusion in separate storage filaments, it's low viscosity profile, and it's time to gelation of 30 minutes after mixing. Furthermore, it was observed experimentally that the individual components of the two-part Cycom 823 were sufficiently robust to survive the host laminate curing process (120°C for 1 hour) after infiltration into the hollow filaments within the fibre stack

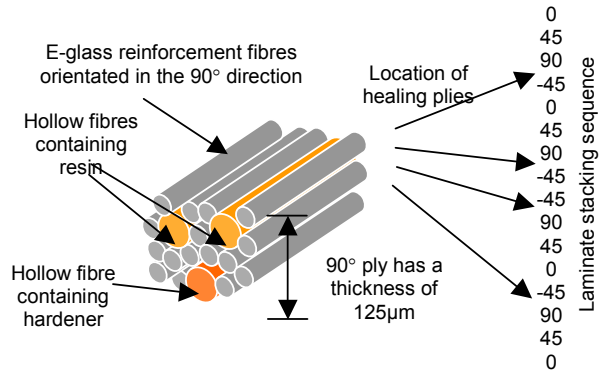


FIG.2 Location of Resin and hardener hollow fibres within the composite laminate

Panels of $200\text{mm} \times 200\text{mm} \times 2.5\text{mm}$ were prepared according to the manufacturer's instructions. Each panel was then sectioned into coupons $20 \text{mm} \times 50 \text{mm}$ for testing. After cutting, the edges of the samples are sealed with a two-part rapid curing epoxy system (Araldite Rapid) to prevent any healing resin loss through the exposed ends of the hollow fibres.

2.2. Self-healing CFRP laminates

It is imperative that any embedded HGF does not detrimentally affect the innate mechanical performance of a FRP, but provides a sufficient volume of healing resin to address any damage. Thus, the incorporation of HGF as discrete plies was deemed unsuitable for CFRP laminates as it would effectively produce a hybrid glass-carbon laminate and result in a significant reduction to their outstanding mechanical properties. A less intrusive approach was devised whereby a small number of

individual HGF's were distributed within individual CFRP plies to act as dispersed storage vessels for the healing agent. Therefore, the distribution of HGF within a CFRP laminate poses a problem of balancing disruption of the host laminate architecture against delivery of adequate healing resin.

Pre-impregnated T300 carbon fibre/914 epoxy resin (Hexcel Composites) was selected as the host material as it is widely used in aerospace applications. A quasi-isotropic stacking sequence of 16 plies was prepared as a 230mm x 160mm x 2.5mm plate. Two different HGF distributions (fibre spacing of 70µm and 200µm respectively) were wound directly onto uncured CFRP plies prior to lamination to investigate the effect of HGF on the host laminate properties and the healing efficacy of different healing agent volumes. HGF was located at two 0°/-45° interfaces within the lay-up as follows:

$$(-45^{\circ}/90^{\circ}/45^{\circ}/0^{\circ}/\mathbf{HGF}/-45^{\circ}/90^{\circ}/45^{\circ}/0^{\circ} // \\ 0^{\circ}/45^{\circ}/90^{\circ}/-45^{\circ}/\mathbf{HGF}/0^{\circ}/45^{\circ}/90^{\circ}/-45^{\circ})$$

The inclusion of HGF within the CFRP stack was such that short lengths (10-20mm) of exposed HGF protruded from the panel edges. This facilitated the vacuum assisted infiltration of the HGF after cure of the laminate with a two-part epoxy resin healing agent (Cytec Cycom823) immediately prior to testing.

2.3. Vascular self-healing system

Sandwich cores were manufactured from 52kg/m³ Rohacell polymethacrylimide closed-cell foam. A schematic representation of the manufacture process for samples containing a vascular network is shown in figure 3, and is described in more detail in this section.

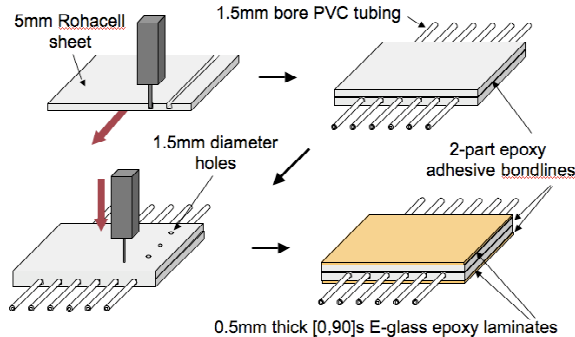


FIG. 3 Manufacture of vascular sandwich panels.

Initially, two half cores of 5mm thickness were used. Straight channels 2mm wide and 2.5mm deep were machined into one of the half cores. PVC tubing of 1.5mm internal and 2.5mm external diameter (Altec Ltd, UK) was laid into the channel after adhesive had been spread over the surfaces of both surfaces. The total resin coverage appropriate to produce a consistent midplane bond using this manufacture technique was found to be 1390g/m². Corebond 340 (SPSystems, UK) was selected on the

basis of material properties, capacity for room temperature cure and high viscosity to avoid open channels becoming filled with resin during later processing stages. The centreline bond was oven cured in a vacuum bag at 60°C for 5 hours; the cure temperature was selected to limit deformation of the PVC tubing. This produced a core of 10.5mm thickness that appeared as a conventional core, but incorporated vessels close to the midplane. To form the network of risers, 1.5mm holes were drilled through the core and tube at appropriate locations. Additional Corebond 340 adhesive was applied to plug the exposed holes and allowed to gel for 24 hours at 20°C to seal the network for the subsequent stages. After this time the plugs were solid enough to be manually sanded flush with the surface of the core in preparation for bonding to the skins. Composite skins 300mm square of [0,90]_s layup and 0.5mm nominal thickness were prepared from pre-impregnated E-glass/913 epoxy (Hexcel, UK) using the recommended autoclave cure cycle. The top face of each plate was then sanded using P120 grit silicon carbide paper and lightly solvent cleaned using acetone. The skins were bonded to the core using Corebond 340 (SPSystems, UK) at 830g/m². This was also spread over both surfaces to ensure a consistent bond with minimum bonding pressure. To minimise the risk of the network becoming filled with resin, the skin bonding operation was completed at room temperature for 24 hours under deadweight pressure of approximately 2.8kN/m². A post-cure of 60°C for 5 hours was then applied to the whole panel to enhance the performance of all the bond lines. A schematic representation of a vascular sandwich panel designed for a two-part resin system, along with the four-point bend flexural test setup is shown in figure 4.

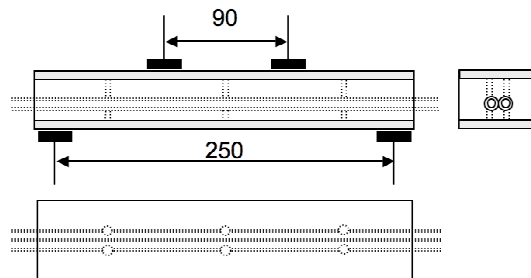


FIG. 4 Schematic representation of a two-part vascular network sandwich beam and four-point bend test setup. Not to scale.

3. MECHANICAL TESTING

3.1. Self-healing GFRP laminates

Four-point bend flexural strength testing according to ASTM D6272-02 was selected to characterise the strength of standard GFRP and self-healing specimens. This configuration ensures a region of uniform bending stress in the area of the damage between the loading noses. A support span to depth ratio of 32:1 and a support span to load span ratio of 3:1 were selected. Six repeat tests were conducted using a loading rate of 5mm/min on a Roell Amsler hydraulic test frame fitted with a 25kN load cell. A Linear Potentiometric Displacement Transducer (LPDT) was used to record mid-span deflection, which

was logged through a PC running Instron data acquisition software.

In the case of the damaged specimens, a three-point bend indentation test using a hardened steel hemisphere of 4.63 mm diameter with the specimen back face supported by a steel ring (OD = 34mm, ID=19mm) was used to create repeatable damage. A peak load of 2500N was used to initiate matrix shear cracks and delamination within the laminate. In the case of the laminate containing the self-healing specimens this was permitted to heal by heating to 100°C (from ambient) in an air circulation oven and held at this temperature for 2 hours. This heating was acceptable as it allowed some degree of control during the study and matched the environment of the intended aerospace application.

Specimen description	Flexural strength [MPa]	% retained strength
Control laminate - no damage	668 ± 13	100
Self-healing laminate - no damage	559 ± 12	84
Control laminate – damaged (2500N peak load)	479 ± 32	72
Self-healing laminate – damaged, no repair	494 ± 7	74
Self-healing laminate – damaged + 2 hrs at 100°C	578 ± 28	87

TAB. 1 Summary of flexural strength and healing efficacy for GFRP

The results in Table 1 indicate that the inclusion of HGF imparts an initial strength reduction of 16%. The control laminate and self-healing laminate with no healing had comparable damage tolerance both in terms of damage size and residual failure strength (typically 72-74%). After healing it was found that a laminate had a residual strength of 87% compared to the undamaged control and 100% compared to an undamaged self-healing laminate albeit with greater standard deviation.

3.2. Self-healing CFRP laminates

As detailed in section 2.2 above, the configuration and manufacture of self-healing CFRP was somewhat different to the GFRP. Ten specimens (100mm x 20mm x 2.5mm) were cut from a plate with the use of a water-cooled diamond grit saw. The sample edges were polished with SiC paper (P2500) to avoid any unwanted edge effects. Samples were then dried, sealed in sample bags and stored in a temperature and humidity controlled environment prior to testing. Immediately prior to commencing any mechanical testing, the HGF within each specimen were infiltrated, using a vacuum assist technique, with pre-mixed, two-part epoxy healing resin (Cytec - Cycom 823).

Quasi-static impact damage was imparted to each specimen using a hardened steel 5mm spherical indenter supported by a steel ring of 27mm outer diameter and 14mm inner diameter mounted on a Hounsfield H20K-W electromechanical test machine. Different load levels were

used to introduce an indentation representative of barely visible impact damage (BVID) into the composite laminate. The indentations were stopped at a peak load of either 1700N or 2000N. Up to this point the damage is contained within the laminate and can be likened to BVID, as the impact surface suffers a minor indent and the back face experiences minimal distortion due to back face delamination.

After indentation, the specimens were subjected to 70°C for 45 mins to reduce healing resin viscosity (25cps) and facilitate infiltration into damage sites, followed by cure at 125°C for 75 mins. Whilst this process diverges from the original aim of achieving autonomic healing, the use of a premixed resin and elevated temperature is an attempt to mitigate some of the shortcomings of the Cycom 823 and attempt to demonstrate the greatest healing efficiency possible with this system. No resin system exhibiting all desirable attributes (i.e. low viscosity, insensitivity to mix ratio, rapid cure under ambient conditions and unlimited shelf life) is currently available. However, from a practical perspective, temperature activation provides excellent control of cure initiation, eliminating time constraints on the testing/manufacturing process.

Four-point bend flexural testing (ASTM-D6272-02) was again used to assess the self-healing efficiency of the resulting CFRP. A support span to depth ratio of 32:1 and a support span to load span ratio of 3:1 were selected. Results were obtained from 10 undamaged, 5 damaged and 5 healed specimens. An Instron 8800 controller/data-logger was used to control the test machine and record data. Specimens were monitored to ensure a consistent failure mode and optical microscopy used to record detailed observations.

The results of the four point bend flexural testing are shown in Table 2. This compares the performance of undamaged, damaged and healed specimens for the two HGF pitch spacings alongside a control CFRP laminate with no HGF.

Analysis of Table 2 shows that the 70µm fibre spacing resulted in the largest reduction in undamaged strength (8%). This can be attributed to a significant disruption in fibre architecture (see Figure 5 below). However, after a quasi-static impact at 2000N peak load, this configuration exhibited a significant amount of damage tolerance compared to the 200µm fibre spacing and control laminates. The large volume fraction of HGF also provides a considerable reservoir of healing agent as shown by a 97% recovery of undamaged strength (equivalent to 89% of the undamaged strength of the control laminate).

The 200µm HGF spacing specimens exhibit little reduction in undamaged strength (2%) attributable to the reduced disruption to the host laminate (see Figure 6 below). These specimens behaved similarly to the control laminate when damaged, presumably due to the limited amount of HGF available for crushing. However, healed samples achieved 82% of their undamaged strength (equivalent to 80% of the undamaged strength of the control laminate), despite the significantly lower volume of available healing resin.

Both HGF spacings investigated (70µm and 200µm) show similar trends, experiencing an initial reduction in flexural

Specimen Type		Undamaged (S.D)	Damaged (S.D)		Healed (S.D)	
			@1700N	@2000N	@1700N	@2000N
Control CFRP	Strength [MPa]	583.3 (13.4)	538.6 (55.5)	405.0 (65.5)	-	-
	% of baseline undamaged	100%	92%	69%	-	-
HGF spaced @70µm	Strength [MPa]	534.9 (12.6)	527.3 (8.0)	443.7 (47.4)	529.0 (16.7)	519.6 (28.8)
	% of baseline undamaged	92%	90%	76%	91%	89%
HGF spaced @200µm	Strength [MPa]	568.8 (18.6)	490.1 (31.9)	401.0 (52.9)	523.4 (19.1)	466.6 (21.8)
	% of baseline undamaged	98%	84%	69%	90%	80%

TAB. 2 Summary of flexural strength and healing efficacy for self-healing CFRP

strength in the undamaged state compared to an unmodified control. This can be attributed to three effects:

- 1) Distortion of the reinforcing fibre architecture
- 2) Generation of resin rich regions (crack nucleation/propagation sites)
- 3) Displacement of reinforcing fibres with non-structural HGF (reduction in carbon fibre volume fraction)

3.3. Vascular self-healing system

In order to assess the comparative mechanical performance of conventional sandwich beams and those containing a vascular network, a range of sandwich configurations were prepared and subject to flexural testing. Six conventional sandwich beams were sectioned from a larger panel. The midplane bond and vascular network was eliminated from these samples by using a 10.5mm thick, one-piece Rohacell core.

Three specimens of each of these configurations were manufactured from two 300mm square panels, each sectioned into nine specimens 30mm in width. Samples were conditioned at 20°C for at least 24 hours before flexural testing. Beams were tested in four-point bending according to ASTM C393 on a Roell Amsler vertical axis test machine with a 25kN load cell. Four-point bend testing was undertaken with a support span of 250mm chosen to promote skin driven flexural failure modes in the later work on impact damaged specimens. A loading span of 90mm was selected to give maximum clearance from the damage zone that would be introduced in later specimens. This was the maximum clearance allowed by the geometry of the test fittings. Testing was performed under displacement control at a test speed of 2mm/min. Square load spreaders of 30mm width with flexible pads were used to distribute the load to prevent localised failure under the loading noses. All samples failed by core shear

approximately midway between the loading and support points.

The structural failure stresses are shown in figure 5 expressed as skin compressive stresses at failure for comparison purposes. In the undamaged and healed cases the failure mode is by a core shear yielding and then fracture; the ultimate load is taken as the point of failure. In the damaged specimens the buckling load has been taken as the point of failure; this has been taken as the point of first significant load fall or the knee in the curve in cases where there is no distinct fall. It is accepted that these loads could be considered somewhat arbitrary but they represent a good indication of the first point at which the structural performance of the specimens has been severely compromised.

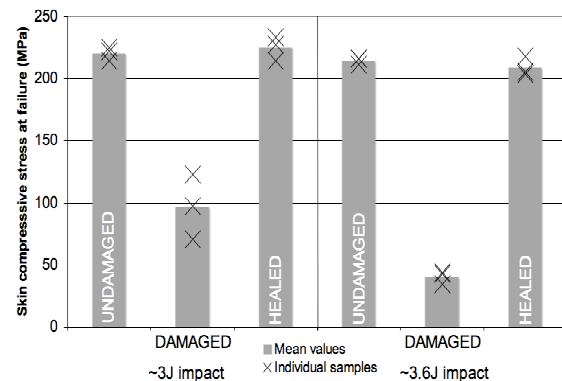


FIG. 5 Summary of mechanical performance of beam specimens. Healed specimens infiltrated with pre-mixed resin

4. LAMINATE MICROSTRUCTURE AND DAMAGE ANALYSIS

Specimens from different test panels were sectioned and polished for microstructural examination. This provided a visual assessment of the disruption caused by the different HGF configurations on the host GFRP and CFRP laminates and identified any inconsistencies present. Furthermore, it provided images to accurately determine the mode of damage propagation through the material.

4.1. Self-Healing GFRP

A damaged and healed GFRP specimen was examined to determine whether healing resin had infiltrated the damage zone. A cross-section of the healed damage illuminated under UV light is shown in Figure 6 which clearly illustrates the extent of the infiltration by the healing resin into the damage zone when viewed along the 0° fibre direction. This result suggests that the four self-healing layer locations were ideally placed within the complex damage network to fully infuse the damage site. To understand the mechanism involved in the self-healing of the damage zone further microscopic examinations were undertaken. This examination indicated the occurrence of crushed hollow fibres under the impact zone (Figures 7a and 7b) and healing resin bridging fracture surfaces (Figures 7c and 7d).

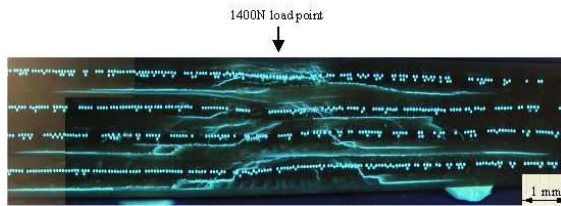


FIG. 6 Impact damaged cross-section of $[0^\circ/+45^\circ/90^\circ/-45^\circ]_2s$ GFRP laminate containing healing filaments at the $+45^\circ/90^\circ$ and $-45^\circ/90^\circ$ interfaces.

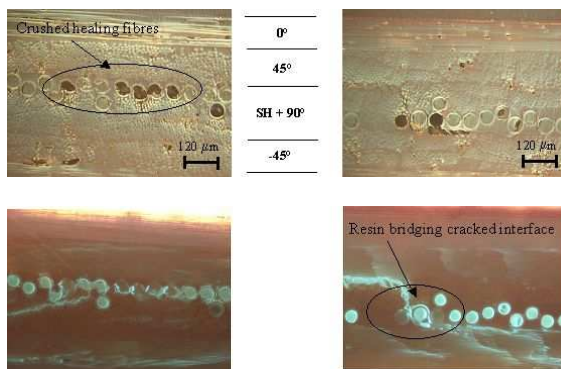


FIG. 7 Crushed-healing fibres located under the impact site viewed under normal (a) and UV (b) illumination. Healing resin bridging cracked interface viewed under normal (c) and UV (d) illumination

4.2. Self-Healing CFRP

A fibre spacing of 70µm (Figure 8) highlighted several issues about the resulting quality of embedding HGF within a laminate. This small pitch spacing was selected to ensure the HGF were in close proximity and thereby facilitate a high degree of healing efficiency. However, during preparation, HGF could be mislocated resulting in disruption to the host ply (Figure 8b). This was attributed to fluctuations in the fibre pitch control at low HGF spacing combined with poor tackiness of the 914 epoxy resin at ambient temperature. This was seen to result in lengths of HGF detaching from and reattaching to the surface producing fibre clumping and resin rich regions post-cure.

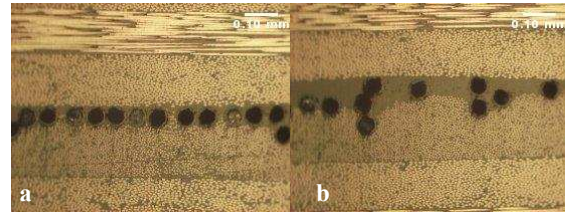


FIG. 8 HGF spaced at 70µm showing (a) good embedment and (b) fibre clumping within host laminate

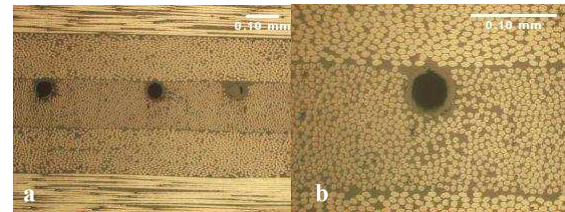


FIG. 9 HGF spaced at 200µm showing (a) consistent spacing and (b) excellent embedment within host laminate.

A fibre spacing of 200µm resulted in a much higher integrity laminate (Figure 9). The resin rich regions surrounding the HGF are minimised and there was no evidence of fibre clumping. The large spacing between fibres allowed the low tackiness of the 914 resin system to hold them in place, any that did detach were able to reattach without interfering with neighbouring fibres. The large spacing between HGF permitted excellent consolidation during cure further improving overall HGF embedment and reducing disruption to the laminate.

Microscopic analysis of samples after quasi-static indentation highlighted the mode of damage development and the interaction with the HGF. The cross sectional damage distribution was typical of an impact damage event. A localised 'crushing' zone was evident on the upper surface followed by shear cracks and delaminations of increasing length through the thickness of the laminate culminating in the largest delamination at the back face between the final two plies of the stack.

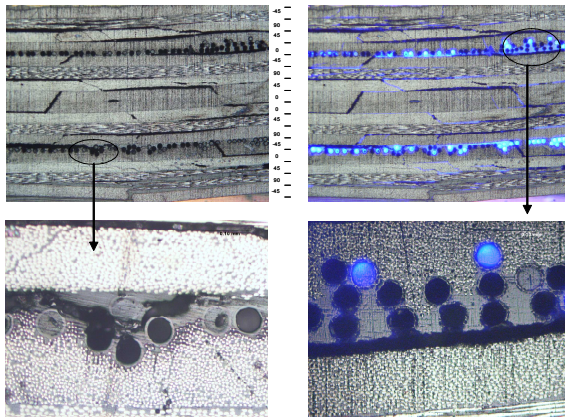


FIG. 10 (a) Damage distribution within laminate (top left), (b) damage infiltration with healing resin and fluorescent dye (top right), (c) delaminations deviating from interface (bottom left) and (d) propagating along interface causing HGF fracture (bottom right).

The process of self-healing is reliant upon the occurrence of two phenomena:

- 1) HGF fibre fracture initiated by a damage event
- 2) Connectivity between HGF and damage network within material

The region of HGF immediately under the impactor was subject to 'crushing' forces, the consequences of which were difficult to discern clearly using optical microscopy. However, the majority of HGF fracture within the laminate is evident from Figure 10a where shear cracks and delaminations are seen to intercept regions of HGF. Furthermore, Figure 10b shows similar damage infiltrated with healing resin mixed with fluorescent dye. It can be seen from this image that the larger delaminations ($>30\mu\text{m}$) contain little or no healing resin. This could be due to the inability of capillary action alone to draw significant volumes of resin into the relatively wide cracks, combined with the limited lengths of HGF available for delivery of resin (test specimen width provided $\sim 40\text{mm}$ HGF length adjacent to damage site).

As expected, delaminations were observed to propagate along interfaces between plies of dissimilar fibre direction. It can be seen that this initiates HGF fracture via two mechanisms.

In Figure 10c, clusters of HGF cause deviation of a delamination, presumably due to a fibre cluster and the resulting resin rich region causing a weakness in the laminate. However, the propagating crack passes directly through HGF causing fibre rupture and release of healing resin. In Figure 10d, HGF are ruptured as a delamination propagates along a ply interface. This suggests their fracture toughness is similar to the surrounding epoxy matrix - a desirable situation for encouraging HGF fracture.

The presence of intra-ply shear cracks linking delaminations provide connectivity between different damage sites in the laminate and facilitate healing at multiple interfaces. Shear cracks can be seen to initiate HGF fracture by similar mechanisms to delaminations

(Figure 11). However, the width of shear cracks is generally smaller than delaminations ($\sim 10\mu\text{m}$ compared to $\sim 30\mu\text{m}$) and so encourage a stronger capillary action to transport healing resin.

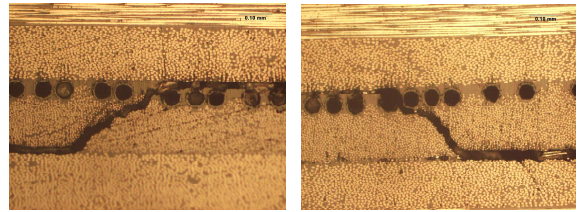


Fig 11 Intra-ply shear cracks intercepting HGF within a self-healing CFRP laminate

The number of fractured HGF depends very much on the severity of the impact and their location within the laminate stack. This provides an ability to tailor for a specific impact energy threshold. In the example shown, approximately 40% of the overall HGF were damaged but with a very uneven distribution throughout the laminate thickness. With regard to the proportion of healing resin which emerges from individual HGF upon fracture, initial studies have shown a range from entire evacuation at gross delamination sites to localised evacuation after matrix cracking. The rate at which a healing agent fills a damage site is a function of the viscosity and the capillary driving force. Once the release and mixture of the two components from adjacent HGF is initiated, the flow into damage sites is offset by an increasing viscosity as the system begins to polymerise. Thus, the infiltration period is limited by the time to gelation i.e. ~ 30 minutes. Post-evacuation, the HGF are still capable of sustaining some load and there is no evidence that empty HGF act to initiate new damage.

4.3. Vascular self-healing system

In sandwich structures real impact damage is clearly subject to significant scatter, however the variation in performance of the damaged specimen at the lower energy level (Figure 5) doesn't detract from the success of the self-healing mechanism because the results suggest that this variability can be addressed successfully by the self-healing mechanism. Figure 12 shows a photograph of the region of damage viewed from the side, and clearly shows the cohesive crack and void in the foam core under the impact site has been filled by healing agent supplied from the vascular network. That this occurred in all samples shows that the rupture of the vertical riser is consistently achieved during impact deformation and confirms that the time required to infiltrate the damage is much less than the time for the resin to cure.

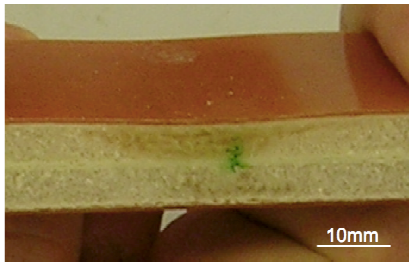


FIG 12 Photograph of a vascular sandwich beam subjected to impact of a 2.8kg cylindrical impactor dropped from 130mm. The damage void has been infiltrated with pre-mixed epoxy resin healing agent through the vascular network in the core.

This study shows that the physical mechanism of using an impact load to rupture channels in the foam which allow healing agent to bleed into the damage is a successful method of initiating self-healing in sandwich structures. Following initiation, the damage zone is successfully infiltrated under only moderate pressures and curing of the resin restores undamaged failure mode and strength.

5. CONCLUSIONS

This work has shown that a hollow-fibre self-healing approach can be used for the repair of advanced composite structures. Hollow glass fibres containing a two-part epoxy healing resin can be manufactured and incorporated within a conventional autoclave processing, indicating that this healing approach can be readily applied to existing composites manufacturing techniques. The specific placement of self-healing plies or individual fibres to match a critical damage threat has been shown to repair internal matrix cracking and delaminations throughout the thickness of a laminate. Such a system offers significant potential in restoring structural integrity to a composite component during service and prolonging residual life after a damage event.

A series of mechanical tests were undertaken to evaluate the influence on the flexural strength of incorporating HGF plies into a GFRP laminate. The results indicate that the inclusion of hollow fibres gives an initial strength reduction, albeit with an increase in damage tolerance. However, after self-healing of an impact damaged laminate it was found that residual strengths of 87% compared to an undamaged baseline non-healing laminate and 100% compared to an undamaged self-healing laminate were achieved.

The incorporation of individual HGF within a CFRP laminate (at fibre spacings of 70 μ m and 200 μ m respectively) has also been shown to produce minimal degradation in flexural strength and disruption to fibre architecture. At fibre spacings of over three fibre diameters (200 μ m), very good embedment of the HGF can be achieved, even on the most demanding 0 $^\circ$ /45 $^\circ$ interface. The presence of uniformly distributed HGF at a ply interface does not appear to cause obvious crack path deviation, suggesting that they do not create sites

of weakness. However, small clusters of HGF combined with resin rich regions can cause significant disruption resulting in crack path deviation. Intra-ply shear cracks and delaminations during an impact event do result in HGF fracture and the release of healing resin into the interconnected damage sites. However, there is evidence to suggest that if crack faces separate by more than 30 μ m, capillary forces may be insufficient, or there may be inadequate resin volume released to fully infiltrate the damage. This inevitably leads towards a system which can provide bleeding under positive pressure to ensure complete infiltration. Overall, these results suggest that bioinspired self-healing is now possible for advanced composite structures.

A simple vascular sandwich structure consisting of horizontal supply channels and vertical riser channels in a closed-cell foam core has been developed. It has been shown that this network has negligible effect on the baseline mechanical properties of the panel. Rupture of a vertical riser containing a pressurised healing fluid can act as a suitable physical initiation for infiltrating the void in the foam core that typically results from blunt impact on composite sandwich structures. The infiltration of a pre-mixed, room temperature curing laminating epoxy restored the undamaged flexural failure mode and failure load of a structure in which impact damage reduced the failure load to 20% of an undamaged specimen.

Further work is currently ongoing to create more realistic damage conditions within the laminates and apply compression after impact (CAI) testing in order to achieve a more rigorous assessment of the effects of HGF on the host laminate and the subsequent healing performance. It is noted, however, that in these studies the healing process is based on a far from optimised healing resin system. Much work remains to be done in developing a healing agent suited to this application, providing controllable initiation on demand, robustness in stoichiometry and longevity in the uncured state. Also, studies are underway with regard to a second generation of self-healing capability in a composite whereby a continuous healing capability is conferred via a vascular network of resin supply.

6. ACKNOWLEDGMENTS

The authors wish to acknowledge the financial support of the European Space Agency and the UK Engineering and Physical Sciences Research Council for funding various aspects of this research under ESTEC Contract No.: 18131/04/NL/PA and Grant No.'s GR/TO3390 and GR/T17984 respectively. The authors would like to acknowledge the funding provided by the University of Bristol through a Convocation Scholarship and Drs Julie Etches and Paul Weaver for useful advice offered in the preparation of this paper.

7. REFERENCES

- [1] Zhou G; The use of experimentally-determined impact force as a damage measure in impact damage resistance and tolerance of composite structures. *Composite Structure*. Vol.42, pp.375-382, 1998.

- [2] Richardson MOW, Wisheart MJ; Review of low-velocity impact properties. *Composites A*. **Vol.27**, pp.1123-1131, 1996.
- [3] Curtis PT; Multifunctional Polymer Composites. *Advanced Performance Materials*. **Vol.3**, pp.279-293, 1996.
- [4] Kassner M E, Nemat-Nasser S, Suo Z, Bao G, Barbour J C, Brinson L C, Espinosa H, Gao H, Granick S, Gumbsch P, Kim K-S, Knauss W, Kubin L, Langer J, Larson BC, Mahadevan L, Majumdar A, Torquato S, van Swol F; *New directions in mechanics. Mechanics of Materials*. **Vol.37**, pp.231–259, 2005.
- [5] Li VC, Lim YM, Chan YW; Feasibility of a passive smart self-healing cementitious composite. *Composites B*. **Vol.29B**, pp.819-827, 1989.
- [6] Dry C; Matrix cracking repair and filling using active and passive modes for smart timed release of chemicals from fibres into cement matrices. *Smart Materials and Structures*. **Vol.3(2)** pp.118-123, 1994.
- [7] Dry C, McMillan W; Three-part methylmethacrylate adhesive system as an internal delivery system for smart responsive concrete. *Smart Materials and Structures*. **Vol.5(3)**, pp.297-300, 1996.
- [8] Chen X, Dam MA, Ono K, Mal AK, Shen H, Nutt SR, Sheran K, Wudl F; A Thermally Re-mendable Cross-Linked Polymeric Material. *Science*. **Vol. 295**, pp.1698-1702, 2002.
- [9] Dry C; Procedures developed for self-repair of polymer matrix composites. *Composite Structures*. **Vol.35(3)**, pp.263-269, 1996.
- [10] Motoku M, Vaidya UK, Janowski GM; Parametric studies on self-repairing approaches for resin infused composites subjected to low velocity impact. *Smart Materials and Structures*. **Vol.8**, pp.623-638, 1999.
- [11] Zako M, Takano N; Intelligent materials systems using epoxy particles to repair microcracks and delamination in GFRP. *Journal of Intelligent Material Systems and Structures*. **Vol.10**, pp.836-841, 1999.
- [12] Bleay SM, Loader CB, Hawyes VJ, Humberstone L, Curtis PT; A smart repair system for polymer matrix composites. *Composites A*. **Vol.32**, pp.1767-1776, 2001.
- [13] White SR, Sottos NR, Moore J, Geubelle P, Kessler M, Brown E, Suresh S, Viswanathan S; Autonomic healing of polymer composites. *Nature*. **Vol.409**, pp.794-797, 2001.
- [14] Kessler MR, White SR; Self-activated healing of delamination damage in woven composites. *Composites A*. **Vol.32(5)**, pp.683-699, 2001.
- [15] Kessler MR, White SR, Sottos NR; Self-healing structural composite materials. *Composites A*. **Vol.34**, pp.743-753, 2003.
- [16] Brown EN, White SR, Sottos NR; Microcapsule induced toughening in a self-healing polymer composite. *Journal of Materials Science*. **Vol.39**, pp.1703-1710, 2004.
- [17] Brown EN, White SR, Sottos NR; Retardation and repair of fatigue cracks in a microcapsule toughened epoxy composite – Part I: Manual infiltration. *Composites Science and Technology*. **Vol.65** pp.2466-2473, 2005.
- [18] Brown EN, White SR, Sottos NR; Retardation and repair of fatigue cracks in a microcapsule toughened epoxy composite – Part 2: In situ self-healing. *Composites Science and Technology*. **Vol.65** pp.2474-2480, 2005.
- [19] Pang JWC, Bond IP; Bleeding composites—damage detection and self-repair using a biomimetic approach. *Composites A*. **Vol.36**, pp.183-188, 2005.
- [20] Pang JWC, Bond IP; A hollow fibre reinforced polymer composite encompassing self-healing and enhanced damage visibility. *Composites Science and Technology*. **Vol.65**, pp.1791-1799, 2005.
- [21] Trask RS, Bond IP; Biomimetic Self-Healing of advanced composite structures using hollow glass fibres. *Smart Mater. Struct.* **Vol.15**, pp.704-710, 2006.
- [22] Hucker M, Bond IP, Foreman A, Hudd J; Optimisation of hollow glass fibres and their composites. *Advanced Composites Letters*. **Vol.8(4)**, pp.181-189, 1999.
- [23] Hucker MJ, Bond IP, Haq S, Bleay S, Foreman A; Influence of manufacturing parameters on the tensile strengths of hollow and solid glass fibres. *Journal of Materials Science*. **Vol.37(2)**, pp.309-315, 2002.
- [24] Brown EN, Kessler MR, Sottos NR, White SR; In situ poly(urea-formaldehyde) microencapsulation of dicyclopentadiene. *Journal of Microencapsulation*. **Vol.20(6)**, pp. 719-730, 2003.
- [25] Rule JD, Brown EN, Sottos NR, White SR, Moore JS; Wax-protected catalyst microspheres for efficient self-healing materials. *Advanced Materials*. **Vol.17(2)**, pp.205-208, 2005.